VOL. 12, NO. 19, OCTOBER 2017 ISSN 1819-6608
ARPN Journal of Engineering and Applied Sciences
©2006-2017 Asian Research Publishing Network (ARPN). All rights reserved.

www.arpnjournals.com

MATHEMATICAL MODEL FOR CALCULATING SCALLOP HEIGHT OF TOROIDAL CUTTER IN FIVE-AXIS MILLING

Hendriko Hendriko
Politeknik Caltex Riau, Pekanbaru, Riau Indonesia
E-Mail: hendriko@pcr.ac.id

ABSTRACT

The scallop height is the most substantial variable in determining the quality of machined surface. Many analytical approacheswere proposed to calculated the scallop height infive-axis milling.Most of them addressed the issue of scallop height for toroidal cutter by approximating the inclined cutting tool using two common primitive geometries, either circle or ellipse.This paper presents an analytical method to calculate the scallop height of toroidal cutter produced by predefined tool path in five-axis milling. The present study was aimed to improve the drawback of the existing method in representing the swept curve of inclined toroidal cutter. In this study, the swept curve was calculated analytically by adopting the method to calculate the grazing point in swept envelope development. The coordinate of intersection point was calculated by using the combination of swept curve algorithm and coordinate mapping equations. The proposed method was successfully used to generate scallop height data for two machining processes with different step over.

Keywords: scallop height, toroidal cutter, grazing toroidal approximation, five-axis milling.

1. INTRODUCTION

Many products, such as mould and dies, are designed with free-form surfaces. Currently, those part surfaces are often produced by five-axis milling. Theoretically, five-axis milling offers better efficiency than three-axis milling in producing complex part surface. In five-axis milling, the tool orientation relative to the workpiece can be controlled by two additional degrees of freedom. However, the additional degrees of freedom created complexity as well as flexibility compared to three-axis milling.

Machining free-form part is normally involving a huge number of tool movements. Consequently, it is both a long and costly process. Considering the time needed for finishing and polishing which could consume as much as 75% of the total machining time [1], therefore, selecting and controlling the cutting conditions and the strategies employed to increase product quality become very important.

In general, there are three parameters that are commonly used to control the accuracy of the machined surface: 1) machining tolerance, 2) scallop height, and 3) surface roughness. In multi-axis milling, scallop height becomes the most substantial component in determining the quality of mahined surface. It is influenced by four factors, 1) cutting tool geometry, 2) tool orientation, 3) part surface geometry, and 4) the distance between adjacent tool path (step over). In order to achieve the expected surface quality, the scallop must be well controlled. However, due to the complexity of the part surface and tool orientation, scallop height is difficult to calculate and it cannot be represented easily. In developing tool path for free-form surfaces, the method to determine the scallop height accurately is still a major challenge.

Many studies developed the method to calculate the scallop height during sculptured surface machining. Most of the proposed method calculated the scallop height usinganalytical approaches. Analytical approachwas used to calculate the cut geometry and scallop height in five axis milling because it was much faster and more accurate when compared to the discrete approaches [2-4]. Several researchers [5-8] have performed the study on the effectiveness of inclined flat end mills in the machining of curved surfaces. The results show that flat-end mill produces smaller scallops as compared to ball-end mill. Other studies [9-13] proposed method for calculating the scallop height for ball-end mill to achieve optimal tool path. Ozturk *et al.* [14] investigated the effect of tool orientation to the scallop height in five-axis milling. Meanwhile [8, 13,15] addressed the issue of scallop height for toroidal cutter by simply assumed that the curvature was constant and cutter geometry was approximated by two common primitive geometry, either circle or ellipse.

Senatore *et al.* [10] represented the tool swept envelope by calculating the effective radius of toroidal cutter due to the inclination angle. Then the scallop height with respect to radius of part surface was calculated and finally the optimal step over can be determined. Others studies [5-12, 15, 16] defined the inclined flat and ball end mills as an ellipse. Mathematically, the shape of swept curves (SV) of inclined flat and ball end mill, which are projected into 2D, can be precisely determined by parametric equation of ellipse curve. However, this approach is not applicable to toroidal cutter. Toroidal cutter is decomposed into cylindrical surface and toroidal surface, consequently, determining the swept curve when the inclination angle existsbecomes much more complicated. This statement will be prooved in the section of Implementation and Discussion.

This paper presents an analytical method to calculate the scallop height of toroidal cutter produced by predefined tool path in five-axis milling. The present study was addressed to improve the drawback of the existing method in representing the swept curve of inclined toroidal cutter. In this study, the swept curve was calculated analytically by adopting the method to calculate the grazing point in swept envelope development. The coordinate of intersection point was calculated by using

VOL. 12, NO. 19, OCTOBER 2017 ISSN 1819-6608
ARPN Journal of Engineering and Applied Sciences
©2006-2017 Asian Research Publishing Network (ARPN). All rights reserved.

the combination of swept curve algorithm and coordinate mapping equations.

2. SWEPT CURVE CALCULATION

Geometrycally, toroidal-end cutter is constructed by two surfaces, cylindrical and toroidal surface as depicted in Figure-1a. However, despite it is constructed by two surfaces, the swept curve was only located on the toroidal surface. The representation of toroidal surface with respect to the tool coordinate system (TCS) was described by the following *equation,*

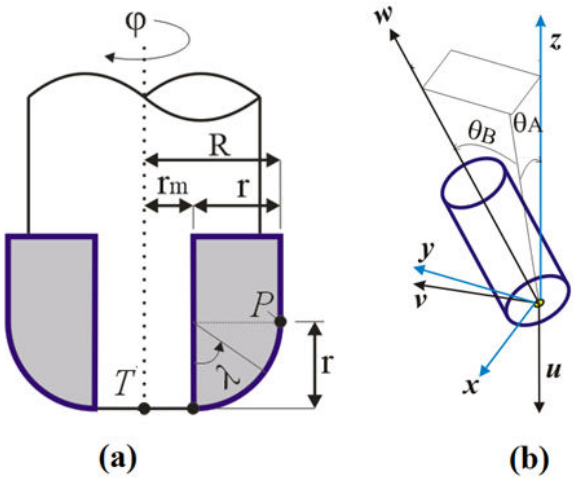

Figure-1. a) Geometry of cutting tool, b) tool orientation due to inclination angle.

$$S_T\,(\varphi;\lambda)\begin{bmatrix}x\\y\\z\end{bmatrix}=\begin{bmatrix}(r_m+r\,sin\,\lambda)\,sin\,\varphi\\(r_m+r\,sin\,\lambda)\,cos\,\varphi\\r-r\,\,cos\,\lambda\end{bmatrix} \quad (1)$$

Where r is minor radius of cutter and r_m is the distance between cutter centre point to the minor radius. Meanwhile λ and φ denotes the toroidal angle and engagement angle, respectively.

In five-axis machining, the tool can be rotated in any direction. Part with sculptured surfaces can be machined efficiently by controlling the tool to move and rotate dynamically with respect to the part surface normal (curvatures). For the purpose of analytical representation of moving surface generation of the cutting tool, appropriate operators of the coordinate system transformations are required. Therefore, three coordinate systems as illustrated in Figure-1 bwere employed to represent the position and orientation of the tool. They are workpiece coordinate system (WCS) which is the reference coordinate frame, tool coordinate system (TCS), and local coordinate system (LCS). To calculate the coordinate transformation, it should be related to a specific machine kinematics. WCS is a fixed frame which is represented by the basis vector x, y, z, while TCS and LCS are denoted by u, v, w and X, Y, Z respectively. The tool inclination angle (α) and screw angle (β) are normally used when a sculptured surface part is machined by five-axis milling. They are the angle formed by TCS and LCS. The operator [M] to map coordinate system from TCS to WCS involving the tool rotation about x-axis (θ_A), y-axis and also translation at T is expressed as follow:

$$[\mathrm{M}]=\begin{bmatrix}cos\,\theta_B & 0 & sin\,\theta_B & x_T\\ sin\,\theta_A sin\,\theta_B & cos\,\theta_A & -sin\,\theta_A cos\,\theta_B & y_T\\ cos\,\theta_A sin\,\theta_B & sin\,\theta_A & cos\,\theta_A cos\,\theta_B & z_T\\ 0 & 0 & 0 & 1\end{bmatrix} \quad (2)$$

On the other hand, the local coordinate frame with orthogonal basis vector u, v, w, which is located at the cutter contact point (CC-point), is defined as,

$$w=\begin{bmatrix}cos\,\alpha & 0 & sin\,\alpha\\ 0 & 1 & 0\\ sin\,\alpha & 0 & cos\,\alpha\end{bmatrix}[0\quad 0\quad 1\,]^T \quad (3)$$

$$\mathrm{v}=\frac{\mathrm{w}\times\mathrm{V_T}}{|\mathrm{w}\times\mathrm{V_T}|}\;;\quad \mathrm{u}=\mathrm{v}\times\mathrm{w} \quad (4)$$

Swept curvewas derived from the method to define grazing point in swept envelope development. As mentioned by [17, 18] that the swept envelope was constructed by three points, forward boundary (egress point), envelope boundary (grazing point) and backward boundary (ingress point). Swept curve was obtained by using the tangency function as follow:

$$F_{(\vartheta,\varphi,p)}=N_{S_T\,(\vartheta,\varphi,p)}.V_{S_T\,(\vartheta,\varphi,p)}=0 \quad (5)$$

where $N_{S_T(\varphi)}$is the cutter surface normal and V_{S_T} is the cutter moving vector. With the same method, every point on the swept curve at every engagement angle is calculated. The normal surface of an arbitrary point Q on toroidal surface in TCS is described by,

$$N_{S_T}=\frac{\partial S_T/\partial\lambda}{|\partial S_T/\partial\lambda|}\times\frac{\partial S_T/\partial\varphi}{|\partial S_T/\partial\varphi|}=\begin{bmatrix}sin\,\lambda\,.\,sin\,\varphi\\ sin\,\lambda\,.\,cos\,\varphi\\ -\,cos\,\lambda\end{bmatrix} \quad (6)$$

When Equation (6) was transformed to the moving frame, it yields to,

$$N_{S_T{}'(\vartheta,\varphi,p)}=sin\,\lambda\,.\,sin(\varphi)\,.\,u+sin\,\lambda\,.\,cos(\varphi)\,.\,v-cos\,\lambda\,.\,w \quad (7)$$

The velocity of an arbitrary point Q on the toroidal surface was determined as follow:

$$V_{S_T}=V_T+\omega\times\overrightarrow{TQ} \quad (8)$$

where ω and $\overrightarrow{TQ}$ denote the angular velocity and the position vector from T to Q, respectively. Since the model was developed by assumed the tool is static, hence there was no angular motion ($\omega=0$). And linear velocity was equal to f ($\mathrm{V_T}=\mathrm{f}$). The tangency function yield to,

©2006-2017 Asian Research Publishing Network (ARPN). All rights reserved.

$$F_{(\vartheta,\varphi,p)} = \sin\lambda.\sin(\varphi).(V_T.u) + \sin\lambda.\cos(\varphi).(V_T.v) + \cos\lambda.(V_T.w) = 0 \quad (9)$$

Due to V_T perpendicular to v, then $V_T.v = 0$. Finally, toroidal angle of the swept point as a function of engagement angle is calculated as follow:

$$\lambda_{(\varphi)} = tan^{-1}\left[\frac{V_T.w}{sin(\varphi).(V_T.u)}\right] \quad (10)$$

After $\boldsymbol{\lambda}_{(\boldsymbol{\varphi})}$ was obtained, the coordinat of swept curve point as a function of engagement angle in WCS was calculated as follow:

$$I_{(\varphi)}(x_I, y_I, z_I) = [M]S_T(\varphi_I; \lambda_{(\varphi)}) \quad (11)$$

3. PATH INTERSECTION POINT

The equation to obtain the intersection point between the swept curve of current cutting path and that of adjacent cutting path, which is called path intersection point (I_C), were derived by referring to Figure-2. Since the tool orientation was set without tilt angle, then, the angle of CC-point (τ) of current cutting path and that the subsequent cutting path were similar. It also made the intersection point located in the middle of point CC_1 and CC_2. The distance of intersection point to CC point (s) and the angle of the CC point relative to the part surface was calculated by,

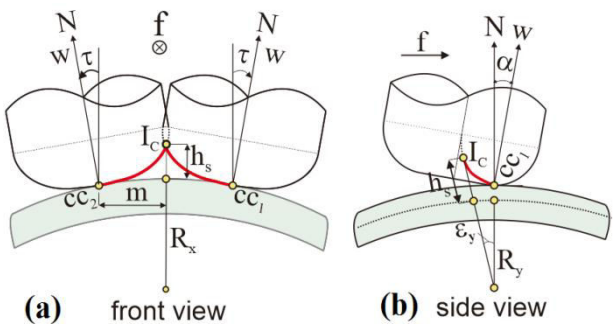

Figure-2. Intersection point of adjacent tool path, a) front view, b) side view.

$$s = |CC_1 - CC_2|/2 \quad (12)$$

$$\tau = \sin^{-1}(s/R_1) \quad (13)$$

where $R_1 = \sqrt{R_x^2 + R_y^2}$. Regarding to the tool rotation by τ, the coordinate of swept point in TCS was mapped to Local Coordinate System (LCS). The mapping of coordinate system was performed by using the following equation,

$$I_C\begin{bmatrix} x_{I_C} \\ y_{I_C} \\ z_{I_C} \end{bmatrix} = \begin{bmatrix} 1 & 0 & 0 \\ 0 & \cos\tau & -\sin\tau \\ 0 & -\sin\tau & \cos\tau \end{bmatrix} \times S_T\ (\varphi_{I_C}; \lambda_{I_C}) \quad (14)$$

The coordinate of $I_C(x_{I_C}, y_{I_C}, z_{I_C})$ could be defined after the toroidal angle of intersection point (λ_{I_C}) was obtained. With respect to LCS, $y_{I_C} = s$. Since y_{I_C} was identified, λ_{I_C} was then defined by extracting Equation (14) only for y_{I_C} as follow:

$$y_{I_C} = \left((r_m + r\sin\lambda_{I_C})\cos\varphi_{I_C}\right)\cos\tau - (r - r\cos\lambda_{I_C})\sin\tau \quad (15)$$

There were two unknown variables exist in Equation (15), λ_{I_C} and φ_{I_C}. Therefore, one of them need to be converted so that only one unknown variable remaining. By rearranging Equation (10), then it was expressed by,

$$\cos(\varphi_{I_C}) = \left[\frac{\sqrt{\left((V_T.u)\sin\lambda_{I_C}\right)^2 - \left((V_T.w)\cos\lambda_{I_C}\right)^2}}{(V_T.u)\sin\lambda_{I_C}}\right] \quad (16)$$

After converting $\cos(\varphi_{I_C})$ in Equation (15) by $\cos(\varphi_{I_C})$ in Equation (16), finally, Equation (15) yielded to become a polynomial equation as follow:

$$(a^2)t^8 + (2ab)t^7 + (2ac + b^2 + f^2)t^6 + (2ad + 2bc)t^5 + (2ae + 2bd + c^2 - f^2)t^4 + (2be + 2cd)t^3 + (2ce + d^2)t^2 + (2de)t + (e^2) \quad (17)$$

where,

$$\begin{aligned} t &= \sin\lambda_{I_C} \\ a &= [(r^2(V_T.u)^2 + r^2(V_T.w)^2)\cos\varepsilon + r^2(V_T.u)^2\sin^2\tau] \\ b &= [2r_m r\cos^2\varepsilon((V_T.u)^2 + (V_T.w)^2)] \\ c &= [(r_m{}^2(V_T.u)^2 + r_m{}^2(V_T.w)^2 - r^2(V_T.w)^2)\cos^2\tau \\ &\quad - (r(V_T.u)\sin\tau + y(V_T.u))^2 \\ &\quad - (r^2(V_T.u)^2\sin^2\tau)] \\ d &= [-2r_m r(V_T.w)^2\cos^2\tau] \\ e &= [-r_m{}^2(V_T.w)^2\cos^2\tau] \\ f &= \left[-2\left(r(V_T.u)\sin\tau + y(V_T.u)\right)(r(V_T.u)\sin\tau)\right] \end{aligned} \quad (18)$$

The roots of polynomial could be easily determined by using software programming such as Matlab. From Equation (17), eight roots of twill be generated. Among those roots, however, only one t that can be converted into λ_{I_C} for obtaining intersection point correctly. The correct one is selected by following these rules, t must be within 0 and 1, if more than one t fulfill the criteria i, then the one that gives $y_{I_C} = s$ will be selected.

Once λ_{I_C} was obtained, then the engagement angle could be determined by using either Equation (10) or Equation (16). The coordinate of PI-point, $I_C(x_{I_C}, y_{I_C}, z_{I_C})$, was defined by using the equation below:

$$I_C(x_{I_C}, y_{I_C}, z_{I_C}) = [M]S_T(\varphi_{I_C}; \lambda_{I_C}) \quad (19)$$

©2006-2017 Asian Research Publishing Network (ARPN). All rights reserved.

Finally, the scallop height ($\boldsymbol{h}$) was calculated by,

$$h = r - r\ cos(\lambda_{I_C}) \quad (20)$$

4. IMPLEMENTATION AND DISCUSSIONS

Based on the formulae derived in the previous sections, a simulation program using MATAB was developed. The proposed method in this study was called Grazing Toroidal Approximation (GTA). In this section the proposed method was tested. In the first test, the proposed method was tested to proof the drawback of the existing swept curve approximations. The second test demonstrates the ability of GTA to calculate the scallop height. Finally, the accuracy of the proposed method was examined by comparing the scallop height obtained using Siemens-NX.

4.1 Grazing toroidal approximation vs ellipse curve approximation

Sample of the swept curve on the cutting tool when the inclination angle exist, and the shape of swept curve projected into 2D was depicted in Figure-3a. Figure-3b compared the shape of the projected curve and ellipse curve for various inclination angle. It can be seen that the shape of projected curve was very dynamic and it cannot be approximated by ellipse when the inclination was small. From a series of test, it was found that the projected curve coincides precisely with ellipse curve when the inclination angle more than 40°. In real machining, however, large inclination angle is avoided. Hence, it proved that ellipse curve approximation method for toroidal cutter tend to produce error.

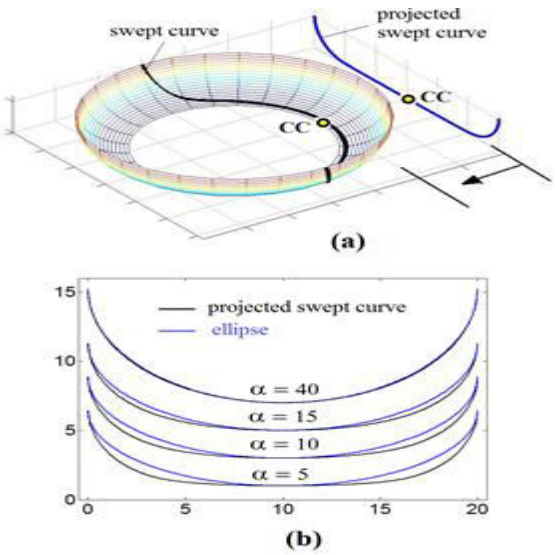

Figure-3. a) swept curve and projected swept curve, b) comparison between ellipse curve and projected swept curve.

4.2 Verification of the scallop height from the GTA

One test using workpiece surface and tool pathas shown in Figure-4a was performed. In this test, the tool was set to perform ramp-up machining process. The inclination angle during the machining process was set decrease gradually as the tool moving up. The machining condition used in the test was feedrate0.3 mm/tooth and spindle speed 5000 rpm. A two teeth toroidal cutter with diameter 20 mm and a minor radius of 5 mm was used as the cutting tool. Using the GTA, the shape of machined surface could be generated. Using the same part model, the machining tests were performed twice with different step over, 5.245 mm and 2.79 mm. The shape of machined surface that were generated by the program simulation are shown in Figure-4b and Figure-4c. From this figure can be seen that the shape of machined surface generated by the GTA resembled the shape of machined surface generated by manufacturing process in Siemens-NX (Figure-4a). This indicates that the proposed method was accurate. The scallop height with respect to cutter contact points (CC-points) are displayed in Figure-4d. From this figure can be seen that increasing the step over will increase the scallop height.

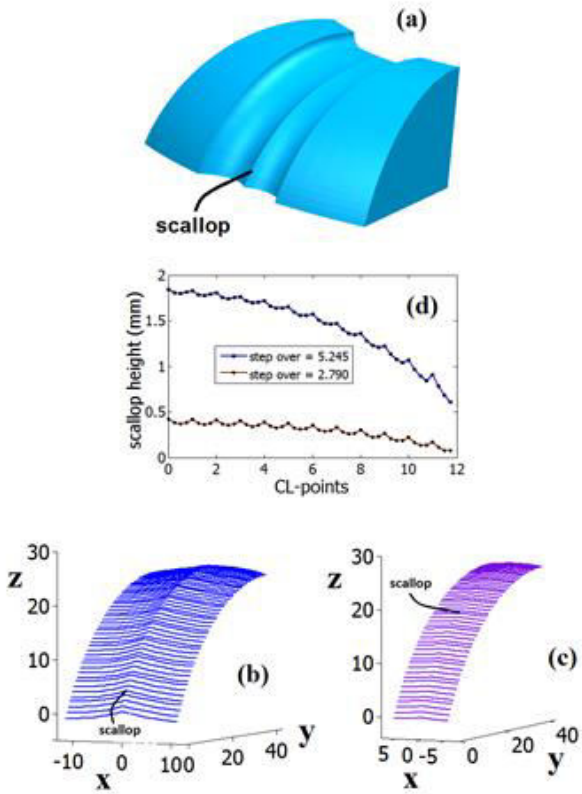

Figure-4. a)Test model, b) scallop progressionwith step over 5.245 mm, c) scallop progression with step over 2.790 mm, d) calculated scallop height.

The method proposed in this study is a part of Analytical Boundary Simulation (ABS) method. In previous studies [2, 4], ABS method was compared with a discrete method in terms of computational time. The results showed that analytical method was computationally more efficient than the Z-mapping method. In this study, the method was proven applicable in supporting the path scallop calculation. This means that the proposed method helps to simplify the work in determining the quality of

©2006-2017 Asian Research Publishing Network (ARPN). All rights reserved.

machined surface in five-axis milling. This is the main advantage of the proposed method compared with other studies based on solid models and discrete methods.

CONCLUSIONS

In this study, a new method, known as the Grazing Analytical Approximation, was developed to generate the scallop height for a toroidal cutter during five-axis milling. The primary contributions of this study include the follow:

a. The proposed method proved that the approximation of inclined toroidal cutting tool using two common primitive geometries, either circle or ellipse is inaccurate.
b. The GTA is applicable to calculate the scallop height of five-axis milling process. It was tested using one-part model with two different step over.

ACKNOWLEDGEMENT

The authors appreciate the funding provided by the Ministry of Research, Technology and Higher Education through the fundamental research grant scheme.

REFERENCES

[1] Mason F. 1995. Die and mold finishing--how fast? Manufacturing Engineering (USA). 115(3): 35-36.

[2] Kiswanto G., Hendriko H. & Duc E. 2014. An analytical method for obtaining cutter workpiece engagement during a semi-finish in five-axis milling. Computer-Aided Design. 55, 81-93.

[3] Hendriko H. 2015. Mathematical model for chip geometry calculation in five-axis milling. Jurnal Teknologi. 77(23).

[4] Kiswanto G., Hendriko H. & Duc E. 2015. A hybrid analytical-and discrete-based methodology for determining cutter-workpiece engagement in five-axis milling. The International Journal of Advanced Manufacturing Technology. 80(9-12): 2083-2096.

[5] Vickers G. W. & Quan K. W. 1989. Ball-mills versus end-mills for curved surface machining. Journal of Engineering for Industry. 111(1): 22-26.

[6] Duvedi R. K., Batish A., Bedi S. & Mann S. 2015. Scallop height of 5-axis machining of large triangles with a flat end mill. Computer-Aided Design and Applications. 12(6): 710-716.

[7] Hricova J. & Naprstkova N. 2015. Surface Roughness Optimization in Milling Aluminium Alloy by Using the Taguchis Design of Experiment. Manufacturing Technology. 15(4): 553-509.

[8] Bedi S., Ismail F., Mahjoob M. J. & Chen Y. 1997. Toroidal versus ball nose and flat bottom end mills. The International Journal of Advanced Manufacturing Technology. 13(5): 326-332.

[9] Feng H. Y. & Li H. 2002. Constant scallop-height tool path generation for three-axis sculptured surface machining. Computer-Aided Design. 34(9): 647-654.

[10] Lin R. S. & Koren Y. 1996 Efficient tool-path planning for machining free-form surfaces. Journal of engineering for industry. 118(1): 20-28.

[11] Wang P., Zhang S. & Yan Z. G. 2016. Study on surface defects in five-axis ball-end milling of tool steel. The International Journal of Advanced Manufacturing Technology. 1-11.

[12] Yigit I. E. & Lazoglu I. 2015. Analysis of tool orientation for 5-axis ball-end milling of flexible parts. CIRP Annals - Manufacturing Technology. 64(1): 97-100.

[13] Warkentin A., Bedi S. & Ismail F. 1996. Five-axis milling of spherical surfaces. International Journal of Machine Tools and Manufacture. 36(2): 229-243.

[14] Ozturk E., Tunc L. T. & Budak E. 2009. Investigation of lead and tilt angle effects in 5-axis ball-end milling processes. International Journal of Machine Tools and Manufacture. 49(14): 1053-1062.

[15] Senatore J., Segonds S., Rubio W. & DESSEIN G. 2012. Correlation between machining direction, cutter geometry and step-over distance in 3-axis milling: Application to milling by zones. Computer-Aided Design. 44(12): 1151-1160.

[16] Wang X. C. & Yu Y. 2002. An approach to interference-free cutter position for five-axis free-form surface side finishing milling. Journal of materials processing technology. 123(2): 191-196.

[17] Chiou C.J, Lee YS. 2002. Swept surface determination for five-axis numerical control machining. Int. J. Mach. Tools and Manuf; 42: 1497-1507.

[18] Weinert K, Du S, Damm P, Stautner M. 2004. Swept volume generation for the simulation of machining processes. Int. J. Mach. Tools and Manuf. 44: 617-628.